

**COMPUTING THE TRAJECTORY OF AN
ARTILLERY SHELL USING SIX DEGREES OF
FREEDOM MODEL**

A PROJECT REPORT

Submitted by

**VISHISH BEHERA [RA1511002010369]
BIBHU PRASAD PADHY [RA1511002010629]
RITURAJ NAYAK [RA1511002010702]**

Under the guidance of

Dr. D. Siva Krishna Reddy

(Research Assistant Professor, Department of Mechanical Engineering)

in partial fulfillment for the award of the degree

of

BACHELOR OF TECHNOLOGY

in

MECHANICAL ENGINEERING

of

FACULTY OF ENGINEERING AND TECHNOLOGY



S.R.M. Nagar, Kattankulathur, Kancheepuram District

May 2019

SRM INSTITUTE OF SCIENCE AND TECHNOLOGY

(Under Section 3 of UGC Act, 1956)

BONAFIDE CERTIFICATE

Certified that this project report titled "**COMPUTING THE TRAJECTORY OF AN ARTILLERY SHELL USING SIX DEGREES OF FREEDOM MODEL**" is the bonafide work of " **VISHISH BEHERA [RA1511002010369], BIBHU PRASAD PADHY [RA1511002010629], RITURAJ NAYAK [RA1511002010702]**" who carried out the project work under my supervision. Certified further, that to the best of my knowledge the work reported herein does not form any other project report or dissertation on the basis of which a degree or award was conferred on an earlier occasion on this or any other candidate.

SIGNATURE

Dr. D. Siva Krishna Reddy
GUIDE
Research Assistant Professor
Dept. of Mechanical Engineering

Signature of the Internal Examiner

SIGNATURE

Dr. S. Prabhu
HEAD OF THE DEPARTMENT
Dept. of Mechanical Engineering

Signature of the External Examiner

ABSTRACT

The present work discusses about computing the trajectory of a projectile using six degree of freedom model. The test case corresponds to 155 mm projectile of Dhanush. Initially Computational Fluid dynamics (CFD) simulations are performed using a commercially available software Ansys-Fluent. Structured grids are used for discretization. Density based solver is used to solve the coupled continuity, momentum and energy equation for various mach number. Further cubic curve fit is done to find the best fit for coefficient of drag as a function of mach number and altitude. The muzzle velocity of the gun is 880m/s fired at an angle of forty five degree. Predicted drag coefficients are validated with the experimental data and error is below five percent. Initially the ballistic code is validated against a published data and the error is around six percent. Next the ballistics of 155 mm projectile are obtained by from the code.

ACKNOWLEDGEMENTS

The success of any project requires involvement of many people and we are fortunate enough to get the support and guidance of the concerned people. We would like to extend our gratitude to the Mechanical Department at SRM Institute of Science and Technology, Kattankulathur and the HOD **Dr. S Prabhu**, for helping and guiding us throughout this project.

We take immense pleasure in thanking our guide project, **Dr. S Siva Krishna Reddy** for his rightful guidance, constant motivation, personal advice, precious time and giving us an outstanding atmosphere for completing the project. We are also grateful to the reviewers of our project for their valuable advice and suggestions. Throughout the work we appreciate their cooperation and continuous support to us in completion of this project work.

VISHISH BEHERA
BIBHU PRASAD PADHY
RITURAJ NAYAK

TABLE OF CONTENTS

ABSTRACT	iii
ACKNOWLEDGEMENTS	iv
LIST OF TABLES	vii
LIST OF FIGURES	viii
LIST OF SYMBOLS	ix
1 INTRODUCTION	1
1.1 Artillery	1
1.2 Ballistics	2
1.2.1 Internal Ballistics	2
1.2.2 External Ballistics	3
1.2.3 Terminal Ballistics	4
1.3 6-Degree of Freedom ballistic model	4
2 LITERATURE SURVEY	6
3 OBJECTIVE AND METHODOLOGY	9
3.1 Objective	9
3.2 Methodology	9
3.3 Computational Fluid Dynamics	10
3.4 Interpolation of Mach Number	11
3.5 Curve Fit	12
3.5.1 Cubic curve fitting with single independent variable	12
3.5.2 Cubic curve fitting with two independent variable	12
3.5.3 Variation of density due to change in altitude	12
3.6 Uncoupled ballistic equation	13

3.6.1	Acceleration	13
3.6.2	Velocity	13
3.6.3	Displacement	14
3.6.4	Angular calculations	14
4	COMPUTATIONAL SIMULATIONS	15
4.1	Mesh	15
4.2	Fluent Simulations	17
4.2.1	Solver Settings	17
4.2.2	Boundary Conditions:	17
5	WIND TUNNEL EXPERIMENTS	18
6	RESULTS AND DISCUSSIONS	20
6.1	Effect of altitude on the Coefficient of Drag	20
6.1.1	Supersonic	20
6.1.2	Transonic	20
6.2	Subsonic Simulations	21
6.3	Contours	21
6.4	Simulation Results	23
6.5	Cubic Curve Fits	23
6.6	Validation of six degree of freedom code	24
6.7	Trajectory of 155mm artillery shell fired from Dhanush Howitzer . .	25
7	CONCLUSION	32

LIST OF TABLES

6.1	Value of Coefficient of Drag at $M=2.07$ at varying altitude	20
6.2	Value of Coefficient of Drag at $M=1.2$ at varying altitude	21
6.3	Simulation Results	23

LIST OF FIGURES

1.1	Drag's effect on the Trajectory of a Projectile.	3
1.2	6 Degrees of Freedom Coordinate System	5
3.1	Profile of 155 mm Artillery	9
4.1	Mesh for Subsonic Conditions	15
4.2	Mesh for Transonic Conditions	15
4.3	Mesh for Transonic Conditions	16
4.4	Boundary Layer Mesh for Supersonic Conditions	16
5.1	Shockwaves seen at Mach No. = 2	19
6.1	P_w/P_{inf} v/s S/D at $M=2.07$	20
6.2	P_w/P_{inf} v/s S/D at $M = 1.2$	21
6.3	P_w/P_{inf} v/s S/D at Subsonic Conditions	21
6.4	Mach Number Contour at $M=0.75$	22
6.5	Mach Number Contour at $M=1.2$	22
6.6	Mach Number Contour at $M=2.07$	23
6.7	Cubic curve fit of C_d as a function of Mach number	24
6.8	Altitude (m) vs Range (m)	26
6.9	Altitude (m) vs Time (s)	26
6.10	Range (m) vs Time (s)	27
6.11	V_x (m/s) vs Time(s)	28
6.12	V_y (m/s) vs Time(s)	29
6.13	Lateral Deflection of the projectile (m) vs Time (s)	30
6.14	Yaw Repose (rad) vs Time (s)	30
6.15	Angle of attack(rad) vs Time(s)	31
6.16	Rate of spin(rad/s) vs Time(s)	31

LIST OF SYMBOLS

ρ	Density
u, v, w	velocity componenets
τ	Shear Stress
$f_{\mathbf{x}}$	Force
e	energy
q	heat
p	pressure
M	Mach Number
V_s	Speed of Sound
$\{\gamma\}$	Heat Capacity
R	Gas Constant
Cd	Coefficient of Drag
a, b, c, d, e	Constants
Y	Altitude
h	Decay Factor
ax, ay, az	Acceleration
g	gravitational acceleration
θ	Pitch angle
β	Side Slip angle
ϕ	Angle between velocity vector and x-axis
D	Diameter
L	Length
P_w	Wall Pressure
P_{inf}	Farstream Pressure

CHAPTER 1

INTRODUCTION

1.1 Artillery

Artillery is a class of expansive military weapons intended to drive huge armory through long distances to make harm to the targets. Artillery's are centered around making mass annihilation causing serious losses and destroying the firmness of the rival. The term artillery is more connected with vast firearm type weapons utilizing a fuel charge to a shoot a projectile along an unguided trajectory.

Between the World War I and World War II the advancement of artilleries started which fundamentally centered around creating greater and heavier weapons which could impel substantial artillery's over longer distances. Advanced artillery has radically developed to concentrate on expanded exactness, mission viability and mechanization. The progressions in the field of artillery has improved to direct the projectiles to give steady and exceptionally exact strikes, augmenting the effect of the gunnery. Despite the fact that the adequacy has improved fundamentally yet a great deal of research must be done to conclusively decide the precise direction of an unguided artillery.

Foreseeing the direction of a ballistic projectile precisely has been contemplated for quite a while. The distinction between the genuine and the anticipated trajectory happens because of different variables like defective part assembling and constant simulation errors. These mistakes make the artillery go amiss from its anticipated path and miss the objective. Thus out-most precautionary measures must be taken while producing the weapon parts and simulations must be checked thoroughly to keep away from any sort of blunder.

Consistent innovative work is being done to improve the precision and stability of the projectile in its path. With maximum stability the range of the projectile can also be increased. As the innovation is improving lighter and increasingly portable artilleries are being made.

1.2 Ballistics

In basic sense, Ballistics is the investigation of the propulsion, flight, conduct and the impact of the projectile. Ballistics has been divided into three kinds: Internal ballistics, External ballistics and Terminal ballistics.

1.2.1 Internal Ballistics

Internal ballistics deals with the projectile's propulsion system. It comprises of the procedures happening when the ballistic projectile is inside the barrel of the weapon. Conventionally, to fire a ballistic projectile the energy required is attained by burning the charges. The present work discusses about computing the trajectory of a projectile using six degree of freedom model. The test case corresponds to 155mm projectile of Dhanush. Initially Computational Fluid dynamics (CFD) simulations are performed using a commercially available software Ansys-Fluent. Structured grids are used for discretization. Density based solver is used to solve the coupled continuity, momentum and energy equation for various mach number. Further cubic curve fit is done to find the best fit for coefficient of drag as a function of mach number. The muzzle velocity of the gun is 880m/s fired at an angle of forty five degree. Predicted drag coefficients are validated with the experimental data and error is below five percent. Initially the ballistic code is validated against a published data and the error is around six percent. Next the ballistics of 155mm projectile are obtained by from the code. for the projectile to be propelled is obtained by igniting the propellants known as charges. The ignition of the charge generates a gigantic measure of force which forces the projectile to be launched into the air and follow its trajectory.

To give more significant stability to the projectile a spinning motion is vital. This spinning motion is given by making inscriptions along the walls of the gun. Ideally, while firing, there shouldn't be any disturbances such as movement occurring in the barrel but due to the forces which occur during the ignition small movements do happen. These movements hamper and adversely affect the accuracy of the projectile.

1.2.2 External Ballistics

External ballistics manages the properties and conduct of the ballistics after it has been propelled into the air. It studies the behavior of the ballistic in its path until the explosions occurs. Coming up next are the forces and phenomena that a projectile experience.

A. Drag

Drag is the resistive power acting the opposite way of the movement of the projectile. At the point when a ballistic projectile is discharged in a vacuum the main power that influences its direction is gravity which acts nearly the equivalent all through the direction. This results in a symmetrical trajectory where the maximum altitude is at half the range. Drag reduces the range of the artillery because of which the greatest height of the projectile would be beyond the half range and the direction would be unsymmetrical. Figure 1.1 depicts the distinction of the trajectory of an artillery in zero drag and with drag conditions.

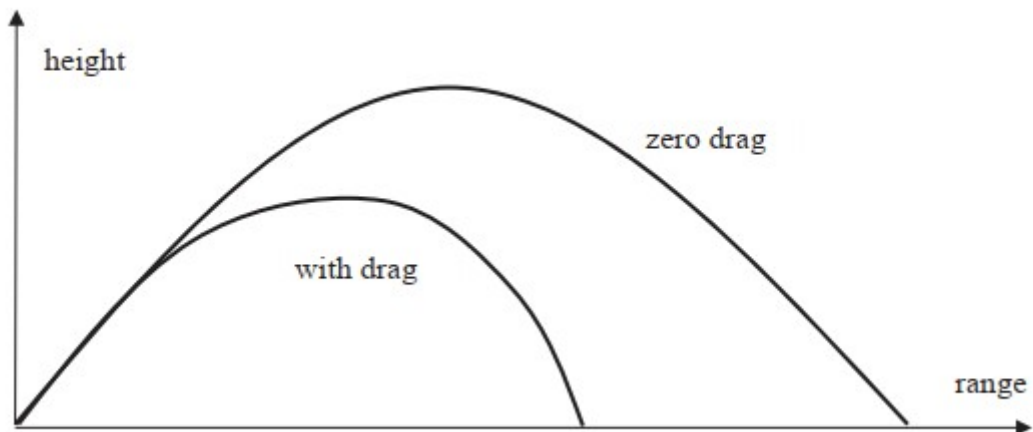


Figure 1.1: Drag's effect on the Trajectory of a Projectile.

There are different sorts of drag. Initially, when the artillery goes through air, it endeavors to push aside and compress the air before it. This compressed air restricts the movement of the artillery. This kind of drag is known as forebody drag. Forebody drag will in general increase with speed. Second, when the air is displaced behind the base of the artillery a low pressure region is produced which makes a halfway vacuum. This is called base drag. Third, the air that surrounds the body of the artillery produces skin

contact further diminishing the speed of the artillery. These are the three types of drag.

B. Stability

The stability of a projectile is very significant in its path of trajectory. The stability can be determined by the position of its center of gravity and center of pressure. For a stable path along the trajectory, the center of pressure must be behind the center of gravity. While considering the design of a ballistic projectile its stability must be considered.

1.2.3 Terminal Ballistics

Terminal ballistics manages the events that happen when the artillery approaches the impact point. Terminal ballistics is the investigation of how a shell carries on when it hits its mark and transmits its energy to the mark. The shell's design and its effect speed determine how well the energy is transmitted. Terminal ballistics is by and large, the least considered part of ballistics while deciding the sort of shell to use for a particular reason. However, it's a significant procedure to comprehend to accomplish ideal outcomes.

1.3 6-Degree of Freedom ballistic model

The report examines the trajectory prediction of 155mm artillery shell utilizing 6 DOF model. A 6-DOF ballistic model is a numerical arrangement that figures the position and axial rotation of the artillery at each point in time. A local and global reference outline is utilized to ascertain the position. Figure 1 depicts the six degrees of freedom the artillery can move in, being x, y, z, I, j and k.

The ballistic model begins with a lot of starting conditions, which are the speed, mass of the artillery, launch angle and the environmental conditions and impacts.

The model created utilizes an iterative procedure whereby the present position and speed is utilized to ascertain the future position. The underlying conditions are incorporated to ascertain the following position, considering a wide range of impacts, for example, gravity, drag and wind. The time-venture between each position can be

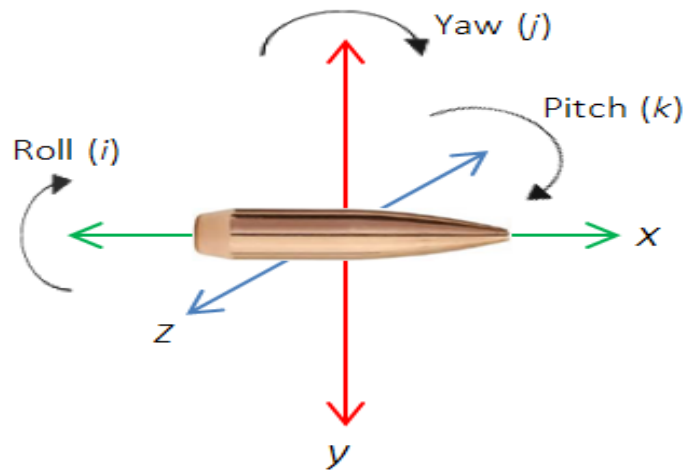


Figure 1.2: 6 Degrees of Freedom Coordinate System

changed to expand the exactness of the model, but by increasing the number of steps, it increases the measure of computational power and time required.

Additionally to a 3-DOF model, a 6-DOF model figures the roll, yaw and pitch of the artillery. This implies the 6-DOF model will be even more exact, as the rotational movement of the artillery impacts the drag and other effects, for example, the Magnus effect. One hindrance that a 6-DOF model has is that it will be slower to assemble than a 3-DOF model, because of greater computational time.

CHAPTER 2

LITERATURE SURVEY

Walter B. Sturek, CharlesJ. Nietubicz^[1], et.al, focuses on the prediction of the aerodynamic characteristic parameters for different projectile models with different configurations. Predictive capabilities which use Navier Stokes computational techniques have been developed and tested on a variety of projectile models to achieve the objective of the report. Code validation and the use of spin stabilizes and fin stabilized projectile shells are described in detail. Healthy progress in the predictive capability of projectile properties is achieved due to the advancement of computational techniques. It emphasizes on constant research and development in the field of computational aerodynamics.

G. R. Cooper and Mark Costello^[2], focuses on methods to analyze the effects of a payload in flight conditions of a ballistic projectile. The payload moments are added with the various forces acting on the shell to examine the trajectory motion. The effects are examined by the use of Navier Stokes equations. To highlight the simulation results an example of ballistic projectile with different payloads are also studied.

Boris Konosevich and Yuliya Konosevich^[3], deal with the movement of an axisymmetric spinning artillery under the influence of aerodynamic forces and conditions as experienced by ballistic models. This paper analyzes the differential equations of the translational and axial rotation of the shell which determines its modified point mass trajectory. Various assumptions and the errors are calculated, and the simulation data are recorded.

Dimitrios N. Gkritzapis^[4], The simulation of a six degree of freedom model with high spin stabilization is examined for the prediction of trajectory of a projectile. It focuses on gyroscopic stability which is very necessary for a stable path of the shell. The computational simulation is done by using the Mach Number and the angle of attack. The yawing and pitching motion are also analyzed for solving the problem. The report mainly focuses on the aerodynamic jump as it has the most importance in

the behavior of the artillery shell trajectory. The results are then verified with the data published in verified reports.

Eric Gagnon and Marc Lauzon^[5], focuses on the control and guidance of unguided artillery shells. It concentrates on course correction models which can be very effective for the performance point of view of the artillery shell and bring down the cost of the overall model. The report is based on 155mm artillery shell. It concludes that spin brake and drag brake concepts are very effective tools to improve the accuracy of the artillery shell. The experimental values are matched with other verified results to validate the results.

M.E. Wessam and Z.H. Chen^[6], present a case study which shows the flow over a model to gain significant knowledge of aerodynamic parameters over the projectile and also about the accuracy of computational models. Software's such as Ansys Fluent and Ansys ICEM CFD were used for the analysis. A modified point mass trajectory model was investigated for precise prediction of trajectory.

K.K. Chand and H.S. Panda^[7], their study attempts to present a single mathematical model to simulate the trajectory of a spin stabilized artillery shell rather than using various other complex models for a conventional artillery shell. It demonstrates how the shape and size of a projectile, and the air resistance affect the prediction of the trajectory. So in order to ease the simulation models the equations of motion have been simplified and the projectile is assumed to be a particle with the only forces acting on them are gravity and drag. With this the trajectory is computed and compared with other validated results.

Nicolas Hamel and Eric Gagnon^[8], In this research paper the authors a deep study was done on aerodynamic properties of 155mm artillery equipped with four canard roll decoupled course correction fuse. In the paper the authors have gone for full body structured mesh and simulations were carried out for various angle of attack using AnsysFluent.

Yongjie Xu, Zhijun Wang^[9], et.al, Six degree model is used to find the design indicators and performance parameters for missile augmentation and design.Active aerodynamics and control systems have been used to the desired results.

John David Stutz^[10], in this paper study of analytical evaluation of trajectories of hypersonic projectiles that are launched into space were deeply done. Further new equation of motion was developed using Keplers equation of motion and decaying factor.

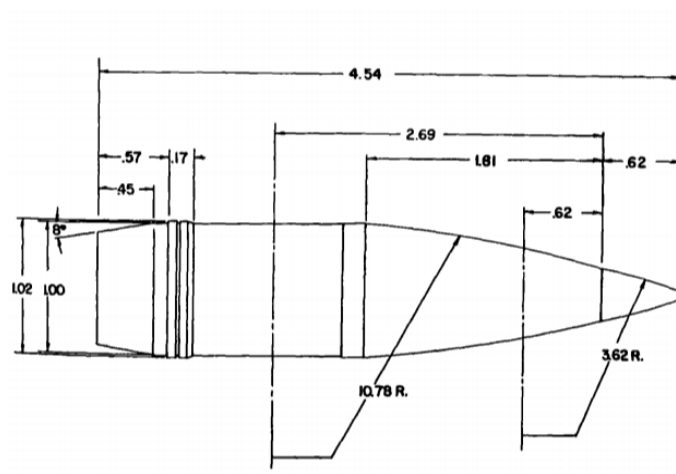
CHAPTER 3

OBJECTIVE AND METHODOLOGY

3.1 Objective

- To perform 2D axi-symmetric simulations over 155mm artillery projectile at supersonic Mach numbers and predict drag coefficients.
- To conduct experiments on scaled model of artillery projectile in supersonic wind tunnel.
- To express drag coefficient as a function of Mach number, angle of attack, altitude using polynomial curve fits.
- To write a code in C language for predicting the trajectory of the shell with 6 Degree of Freedom model.

3.2 Methodology



(All dimensions in calibers)

Figure 3.1: Profile of 155 mm Artillery

We compute the trajectory of an artillery shell of 155 mm diameter, at supersonic conditions considering the variations in drag coefficients. The profile of 155mm artillery shell was taken from the BRL manual. The CAD geometry was made using

SolidWorks. For the purpose of creating the mesh, all dimensions were converted from calibers to mm. ANSYS Fluent is used to generate the mesh with mesh sizing between 1e-3 m and 1e-5 m.

3.3 Computational Fluid Dynamics

We are using Computational Fluid Dynamics as a tool to help compute the Drag Coefficient at different Mach Numbers. The following governing equations are crucial for the simulations:

Continuity equation

Nonconservative form

$$\frac{D\rho}{Dt} + \rho \nabla \cdot \mathbf{V} = 0 \quad (3.1)$$

Conservative form

$$\frac{\partial \rho}{\partial t} + \nabla \cdot (\rho \mathbf{V}) = 0 \quad (3.2)$$

Momentum equations

Nonconservative form

x-component:

$$\rho \frac{Du}{Dt} = -\frac{\partial \rho}{\partial x} + \frac{\partial \tau_{xx}}{\partial x} + \frac{\partial \tau_{yx}}{\partial y} + \frac{\partial \tau_{zx}}{\partial z} + \rho f_x \quad (3.3)$$

y-component:

$$\rho \frac{Dv}{Dt} = -\frac{\partial \rho}{\partial y} + \frac{\partial \tau_{xy}}{\partial x} + \frac{\partial \tau_{yy}}{\partial y} + \frac{\partial \tau_{zy}}{\partial z} + \rho f_y \quad (3.4)$$

z-component:

$$\rho \frac{Dw}{Dt} = -\frac{\partial \rho}{\partial z} + \frac{\partial \tau_{xz}}{\partial x} + \frac{\partial \tau_{yz}}{\partial y} + \frac{\partial \tau_{zz}}{\partial z} + \rho f_z \quad (3.5)$$

Conservative form

x-component:

$$\frac{\partial(\rho u)}{\partial t} + \nabla \cdot (\rho u \mathbf{V}) = -\frac{\partial \rho}{\partial x} + \frac{\partial \tau_{xx}}{\partial x} + \frac{\partial \tau_{yx}}{\partial y} + \frac{\partial \tau_{zx}}{\partial z} + \rho f_x \quad (3.6)$$

y-component:

$$\frac{\partial(\rho v)}{\partial t} + \nabla \cdot (\rho v \mathbf{V}) = -\frac{\partial \rho}{\partial y} + \frac{\partial \tau_{xy}}{\partial x} + \frac{\partial \tau_{yy}}{\partial y} + \frac{\partial \tau_{zy}}{\partial z} + \rho f_y \quad (3.7)$$

z-component:

$$\frac{\partial(\rho w)}{\partial t} + \nabla \cdot (\rho w \mathbf{V}) = -\frac{\partial \rho}{\partial z} + \frac{\partial \tau_{xz}}{\partial x} + \frac{\partial \tau_{yz}}{\partial y} + \frac{\partial \tau_{zz}}{\partial z} + \rho f_z \quad (3.8)$$

Energy equation

Nonconservative form

$$\rho \frac{D}{Dt} \left(e + \frac{V^2}{2} \right) = \rho q - \frac{\partial(u\rho)}{\partial x} - \frac{\partial(v\rho)}{\partial y} - \frac{\partial(w\rho)}{\partial z} + \rho \mathbf{f} \cdot \mathbf{V} \quad (3.9)$$

Conservative form

$$\frac{\partial}{\partial t} \left[\rho \left(e + \frac{V^2}{2} \right) \right] + \nabla \cdot \left[\rho \left(e + \frac{V^2}{2} \right) \mathbf{V} \right] = \rho q - \frac{\partial(u\rho)}{\partial x} - \frac{\partial(v\rho)}{\partial y} - \frac{\partial(w\rho)}{\partial z} + \rho \mathbf{f} \cdot \mathbf{V} \quad (3.10)$$

3.4 Interpolation of Mach Number

Mach Number is the ratio the ratio of speed of the shell to the speed of sound at a certain altitude.

$$M = V/V_s \quad (3.11)$$

$$V_s = (\gamma RT)^{0.5}, \quad (3.12)$$

Where V is the speed of projectile and Vs is the speed of sound.

US standard atmospheric properties are used to calculate the temperature(T) at a certain altitude.

$$T = T_0 - 6.5Y \quad (3.13)$$

3.5 Curve Fit

3.5.1 Cubic curve fitting with single independent variable

The coefficient of drag (C_d) is to be fitted as a function of Mach number (M). The cubic curve fit equation as a function of Mach number is as follow :

$$C_d = a + bM^3 + cM^2 + dM \quad (3.14)$$

Hence four data point are required to fit the the curve.

3.5.2 Cubic curve fitting with two independent variable

In this case the coefficient of drag(C_d) is to be fitted as a function of Mach number(M) and altitude(Y). The cubic curve fit equation as a function of Mach number is:

$$C_d = a + bM^3 + cM^2 + dM^2Y + eMY^2 + fM + gY + hY^3 + iY^2 + jMY \quad (3.15)$$

Hence ten data point are required to fit the curve.

3.5.3 Variation of density due to change in altitude

The variation in density due to change in altitude is as denoted by the following equation:

$$\rho = \rho_0 e^{-hy} \quad (3.16)$$

Where ρ_0 is the density of air at the launch site and h is the decay factor per meter i.e $h = 0.9625 \text{ m}^{-1}$.

3.6 Uncoupled ballistic equation

In order to obtain the trajectory of the shell in six degree of freedom the velocity, distance traveled and angular motion about each axis i.e x,y and z are required to be solved respectively.

3.6.1 Acceleration

The acceleration about each component are derived from Newtons second law of motion with the drag force equation. For horizontal(x), vertical(y) and lateral(z).

$$ax = (-0.5SCdpv^2 \cos(\theta) \cos(\phi)) \quad (3.17)$$

$$ay = g - (0.5SCdpv^2 \sin(\theta) \cos(\phi)) \quad (3.18)$$

$$az = (0.5SCdpv^2 (CNA \sin(\beta) \cos(\phi + \beta) - C \cos(\theta) \sin(\phi))) \quad (3.19)$$

3.6.2 Velocity

$$V_x(t + dt) = V_x(t) + a_x(t)dt \quad (3.20)$$

$$V_y(t + dt) = V_y(t) + a_y(t)dt \quad (3.21)$$

$$V_z(t + dt) = V_z(t) + a_z(t)dt \quad (3.22)$$

The resultant velocity is determined by the following equation:

$$V = (V_x^2 + V_y^2 + V_z^2)^{0.5} \quad (3.23)$$

3.6.3 Displacement

$$x(t + dt) = x(t) + V_x(t)dt \quad (3.24)$$

$$y(t + dt) = y(t) + V_y(t)dt \quad (3.25)$$

$$z(t + dt) = z(t) + V_z(t)dt \quad (3.26)$$

3.6.4 Angular calculations

Using orthogonal velocity components, the angles that are used to resolve the forces and calculate the yaw repose :

Projectile Pitch angle

$$\theta(t + dt) = \tan^{-1} \frac{V_y(t + dt)}{V_x^2(t + dt) + V_y^2(t + dt))^{0.5}} \quad (3.27)$$

Projectile Side slip angle

$$\beta(t + dt) = \frac{8p(t + dt)I_{xx}g\cos\theta(t + dt)}{\pi pD^2LC_{ma}V(t + dt)^3} \quad (3.28)$$

Angle between velocity vector and x-axis

$$\phi(t + dt) = \tan^{-1} \frac{V_z(t + dt)}{V_x(t + dt)} \quad (3.29)$$

Rate of spin

$$p = \frac{2\pi V}{Ld} \quad (3.30)$$

Where V is the net velocity of the projectile,

L is the twist rate of the gun,

D is the diameter of the shell,

Dt is the time step.

CHAPTER 4

COMPUTATIONAL SIMULATIONS

4.1 Mesh

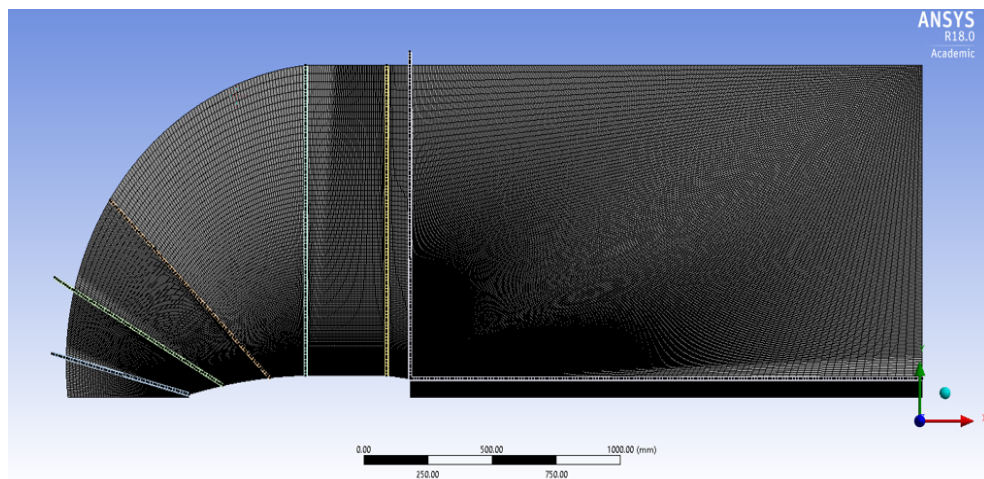


Figure 4.1: Mesh for Subsonic Conditions

Total No. of Nodes = 54120

Total No. of Elements = 50095

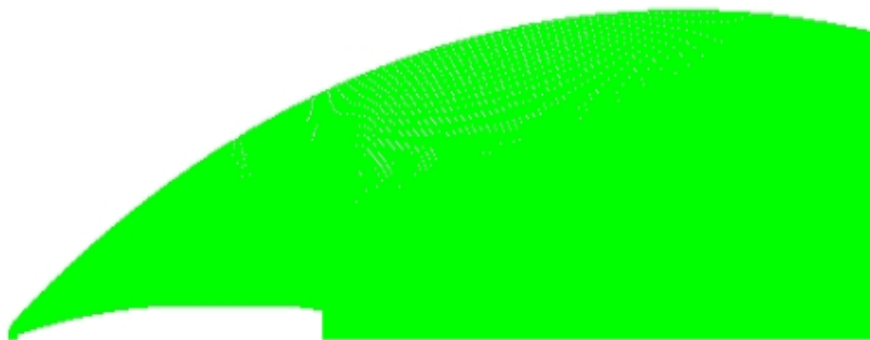


Figure 4.2: Mesh for Transonic Conditions

Total No. of Nodes = 89285

Total No. of Elements = 88400

Biasing = 500

Biasing is used to make the elements more fine near the Artillery Wall.

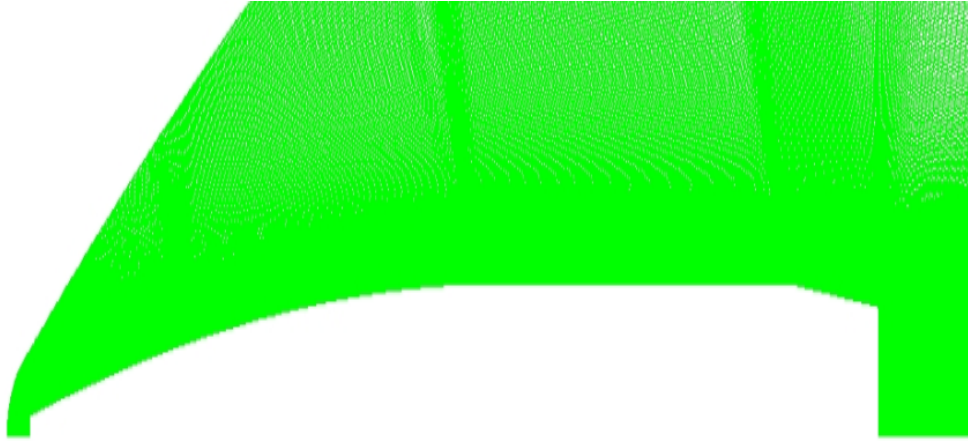


Figure 4.3: Mesh for Transonic Conditions

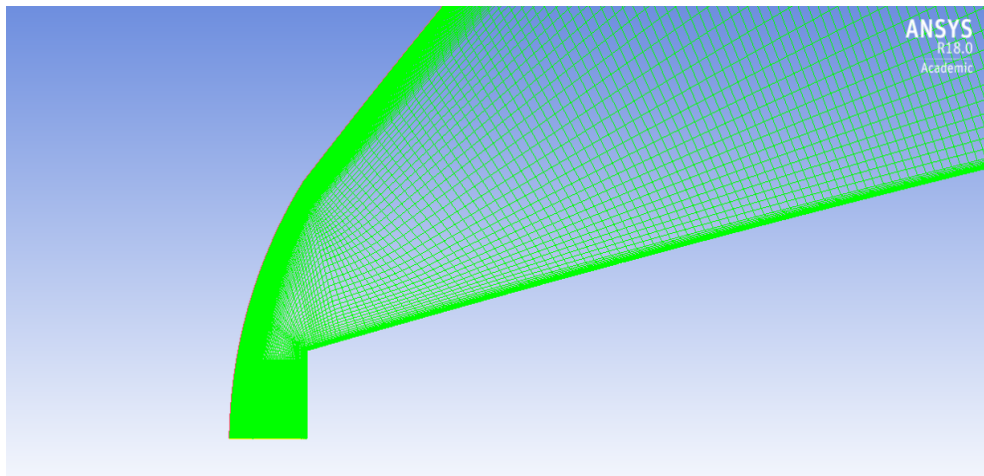


Figure 4.4: Boundary Layer Mesh for Supersonic Conditions

Capturing Shockwaves is difficult as the grid needs to be well aligned, and for each Mach Number in the supersonic regime, the grid needs to be different because when Mach Number increases, the shock wave comes closer to the wall. Hence, Boundary Layer Mesh is fine near the wall (for adjusting the boundary) and near the outer domain (to capture shockwave and adjust the grid with change in Mach Number).

4.2 Fluent Simulations

We have used Ansys Fluent for our simulations for it's ease and user-friendly interface.

4.2.1 Solver Settings

- A Density based solver with steady state time condition and axi-symmetric model is used.
- Energy equation is switched on.
- Standard K-Epsilon Turbulence model has been chosen.
- Ideal gas is used.

4.2.2 Boundary Conditions:

Inlet-

Boundary Conditions - Pressure Farfield

Mach - Ranging from 0.6 to 2.07.

Gauge Pressure - 0 Pascal

Turbulence Intensity = 5%

Outlet-

Gauge Pressure - Atmospheric Pressure

Backflow Turbulent Intensity = 10%

Backflow Turbulent Length Scale = 0.01 m

Artillery Shell-

Boundary Condition - Wall with No Slip Conditions

Explicit Method with AUSM Flux type solver is used.

CHAPTER 5

WIND TUNNEL EXPERIMENTS

Wind burrows are expansive cylinders or passages with air moving inside them. They are utilized to examine the activities of an item in flight. These are extremely compelling methods for deciding the forces acting and conduct of the item progressively flight conditions. The item can be a full scale model or a downsized model depending upon the span of the wind tunnel machine. The air moving around the model helps in figuring out what might occur if the item was moving in air. The progression of Computational Fluid Dynamics (CFD) has decreased the interest for wind tunnel testing, but, anyway the CFD results are as yet not entirely dependable and consequently wind tunnel testing machines are utilized to validate the CFD results. The wind tunnels can be named as subsonic, supersonic and hypersonic.

The supersonic wind tunnel machine was used to validate the results for the successful completion of the report.

Supersonic Wind Tunnel testing was done at Mach No. 2 to check for the shock waves at the nose cone of the model. To lead the test a smaller than normal model of the 155mm artillery shell was made. The small scale model is downsized model of the genuine model with scale down factor of 15. The model was made of hardened stainless steel. The test was done for 2 mins with appropriate mounting and wellbeing methodology. The picture of the shock waves was caught utilizing the Schlieren Flow Visualization approach. Schlieren photography depends on the shadowgraph procedure to get the image of the shock waves. This method utilizes white papers to catch the shock waves in highly contrasting structure.

Specifications of the Wind Tunnel are:

- **Model and Make:** HP 20-300 ELGI
- **Compressor Power:** Each 20 HP (2 nos)
- **Drier:** Silicon Filled
- **Cooler:** Electrically Driven

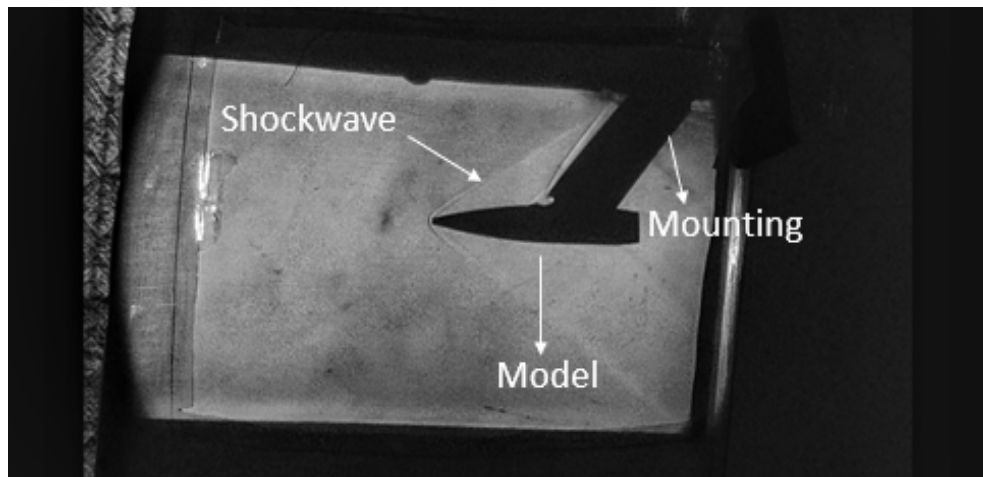


Figure 5.1: Shockwaves seen at Mach No. = 2

- **Test Section:** Frontal Area 100 X 100 mm²
- **Distance from Throat of the Model:** 430 mm
- **Total length of test section:** 640 mm
- **Type:** Blow Down to atmosphere
- **Duration of Running time:** More than 60 seconds

CHAPTER 6

RESULTS AND DISCUSSIONS

6.1 Effect of altitude on the Coefficient of Drag

6.1.1 Supersonic

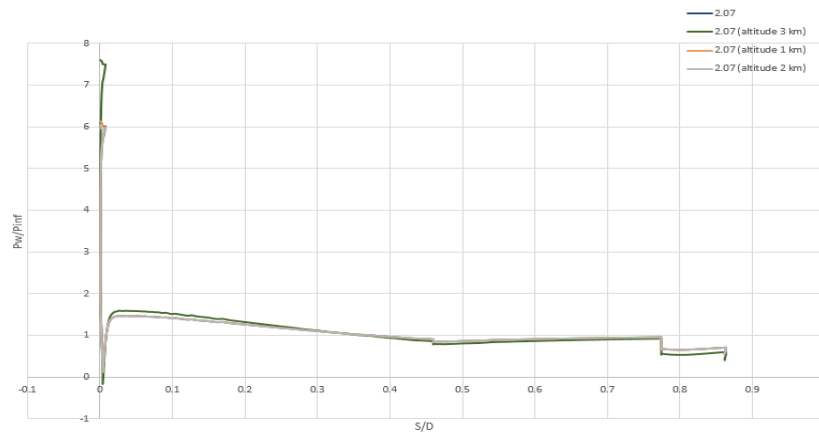


Figure 6.1: P_w/P_{inf} v/s S/D at $M=2.07$

Table 6.1: Value of Coefficient of Drag at $M=2.07$ at varying altitude

Altitude (km)	Cd
0 (sea-level)	0.274
1	0.27126
2	0.2685
3	0.2658

6.1.2 Transonic

As the altitude increases there is a significant drop in the ambient pressure i.e. the atmospheric pressure, also due to increase in the velocity of the shell the dynamic pressure increases. Since the rate of fall of ambient pressure is more than the rate of rise in the dynamic pressure. Hence there is a slight increase in P_w/P_{inf} due to increase in altitude.

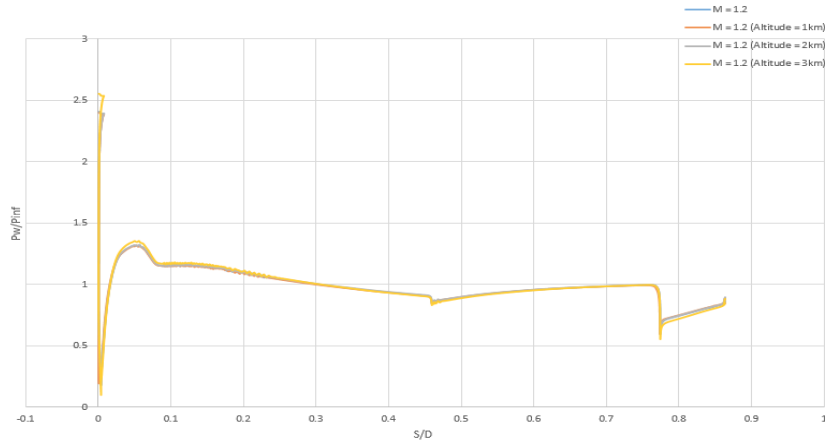


Figure 6.2: P_w/P_{inf} v/s S/D at $M = 1.2$

Table 6.2: Value of Coefficient of Drag at $M=1.2$ at varying altitude

Altitude (km)	Cd
0 (sea-level)	0.364
1	0.36036
2	0.3567
3	0.3532

6.2 Subsonic Simulations

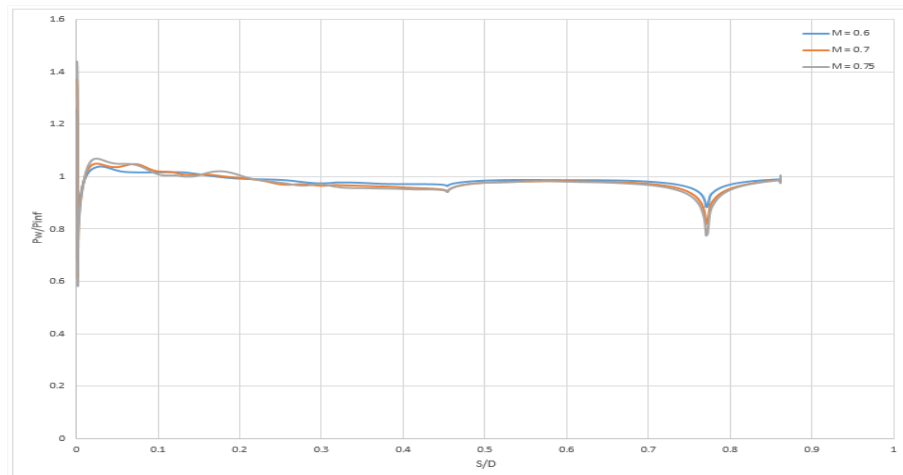


Figure 6.3: P_w/P_{inf} v/s S/D at Subsonic Conditions

6.3 Contours

Below are the contours from the simulations:

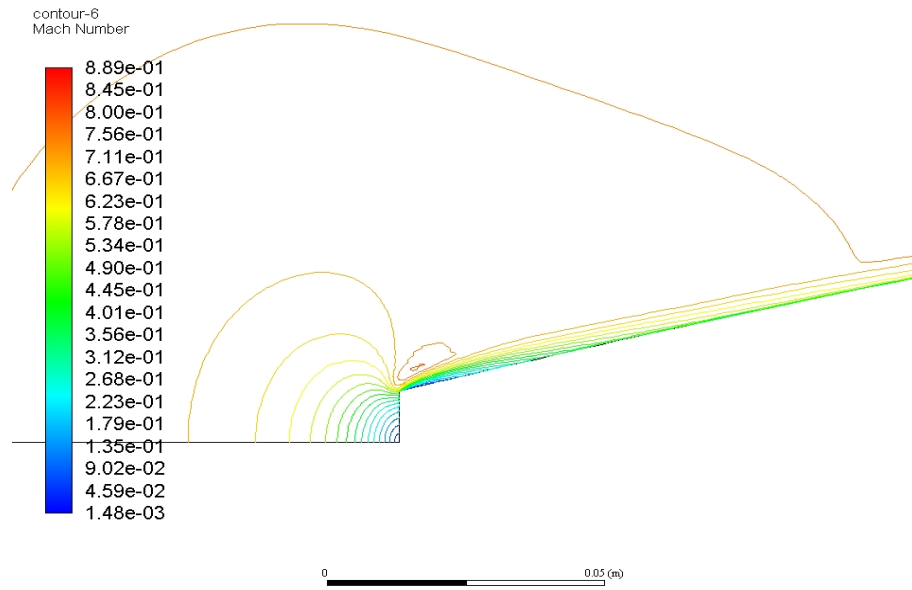


Figure 6.4: Mach Number Contour at $M=0.75$

At subsonic region (Mach 0.75), air is just flowing over the artillery shell.

At $M = 1.2$, shockwaves start developing.

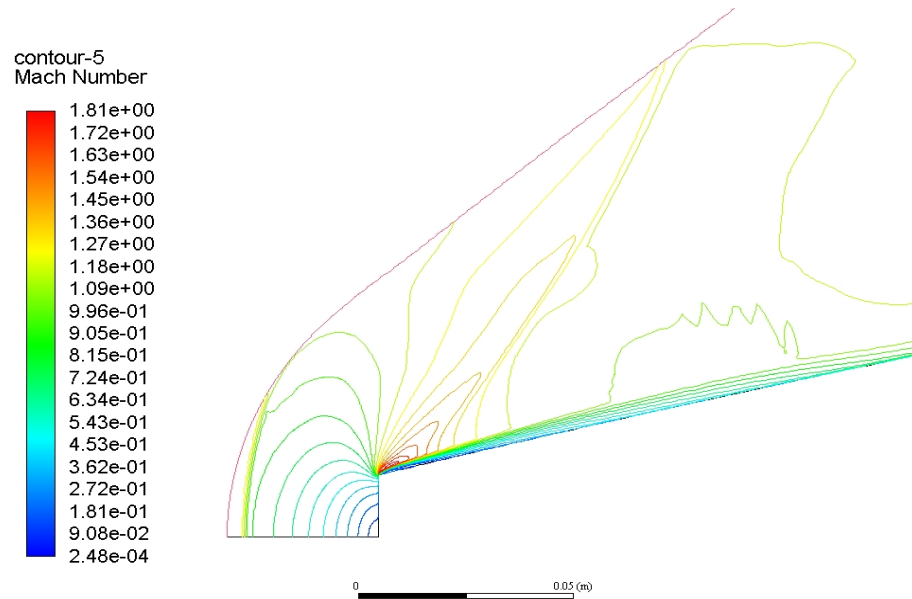


Figure 6.5: Mach Number Contour at $M=1.2$

At $M = 2.07$, the shock wave is clearly visible.

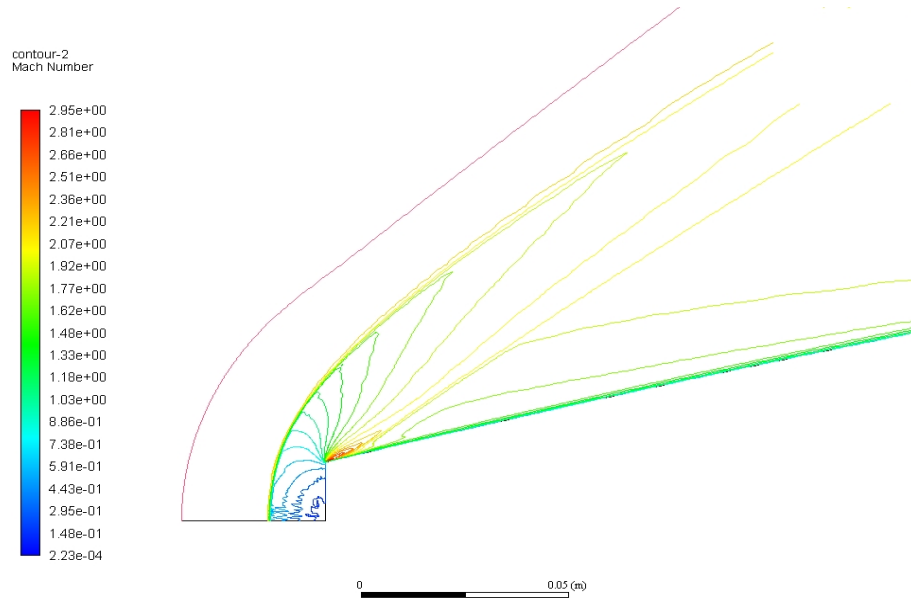


Figure 6.6: Mach Number Contour at M=2.07

Table 6.3: Simulation Results

Mach Number	Cd(Simulation)	Cd(Experiment)	Error
0.6	0.1093	0.107	1.8
0.7	0.1095	0.108	1.38
0.75	0.1097	0.108	1.5
0.8	0.1274	0.1173	2.7
0.98	0.288	0.2970	3.03
1.2	0.364	0.3859	2.4
1.59	0.3031	0.3271	3.64
1.81	0.312	0.3042	2.56
2.07	0.274	0.2829	3.14

6.4 Simulation Results

6.5 Cubic Curve Fits

Similarly cubic curve fit of Cd as a function of Mach number(M) and altitude(Y) are done.

$$Cd = -0.1966 + 0.3761 \times M^3 - 1.1793 \times M^2 + 0.0020 \times M^2 Y + 0.000211307 \times M \times Y^2 + 1.08126835 \times M + 0.0034773Y + 5.947610^{-5} \times Y^3 - 0.000211749 \times Y^2 - 0.004540509 \times M \times Y$$

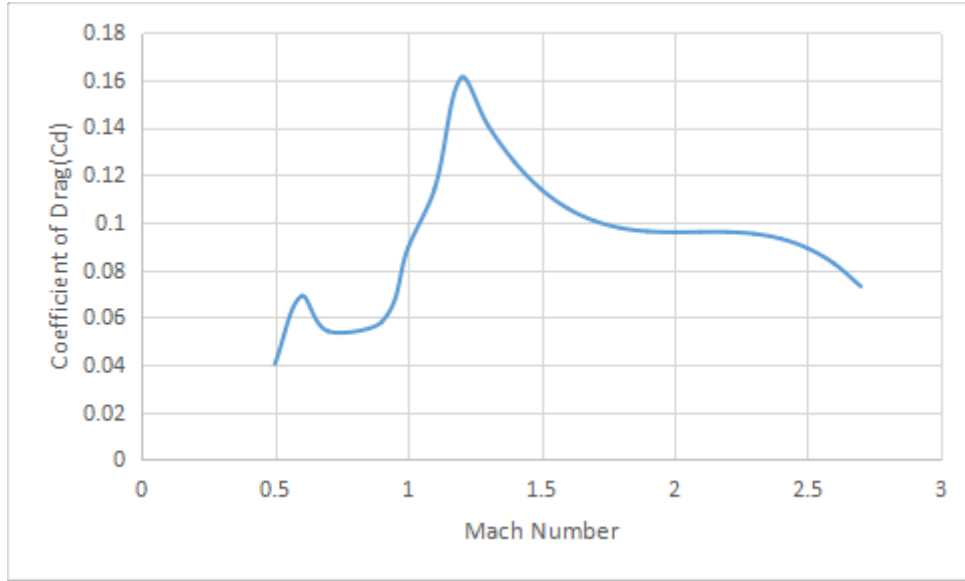


Figure 6.7: Cubic curve fit of Cd as a function of Mach number

$$Cd = -51.4655 - 9.413 \times M^3 - 22.9269 \times M^2 + 10.9676 \times M^2 \times Y + 0.3060428 \times M \times Y^2 + 84.27680425 \times M + 14.51021408 \times Y - 0.004465041 \times Y^3 - 0.26100321 \times Y^2 - 25.59926065 \times M \times Y$$

$$Cd = 1.7325 - 0.0923 \times M^3 + 0.70344 \times M^2 - 0.0414 \times M^2 \times Y - 0.00071443 \times M \times Y^2 - 1.769044 \times M - 0.15455 \times Y + 3.51509 \times 10^{-5} \times Y^3 + 0.000455773 \times Y^2 + 0.16475 \times M \times Y$$

6.6 Validation of six degree of freedom code

The six degree of freedom code is validated by considering a sample problem i.e. Example 9.2^[8].

Physical Characteristics:

- Diameter = 104.8 mm
- Projectile Length = 494.7 mm
- Weight = 14.97 Kg
- Axial Moment of Inertia = $0.023 \frac{kg}{m^2}$
- Transverse Moment of Inertia = $0.231 \frac{kg}{m^2}$
- $C_{Ma} = 3.76$

- The variation in density due to change in altitude as mentioned in **Eq.(3.16)**.
- $C_d=0.27$ (taking it as constant)

Firing Conditions

- Launch Velocity = 493 m/s
- Launch angle = 45degree
- Twist rate 1/18 caliber
- Time step (dt) = 0.1 s

Result^[8]-

The Maximum range of the projectile is 11050m with an error 5.6%. The maximum altitude achieved by the projectile is 3700m with an error of 6.25%. The maximum drift of the projectile is 0.088m with an error of 8%. The total time of flight is 54sec.

6.7 Trajectory of 155mm artillery shell fired from Dhanush Howitzer

Physical Characteristics

- Diameter = 155mm
- Projectile Length = 830mm
- Weight = 43kg
- Axial Moment of Inertia = $0.147 \frac{Kg}{m^2}$
- Transverse Moment of Inertial = $1.893 \frac{Kg}{m^2}$
- $C_{Ma} = 4$
- The variation in density due to change in altitude as mentioned in **Eq.(3.16)**.
- C_d : Cubic Curve Fit presented in **Section 6.5** are used to compute the drag coefficient as a function of Mach Number and Altitude.

Firing Conditions

- Launch Velocity = $880 \frac{m}{s}$

- Launch angle = 45 degree
- Twist rate = 1/18 caliber
- Time step(dt) = 0.1 s

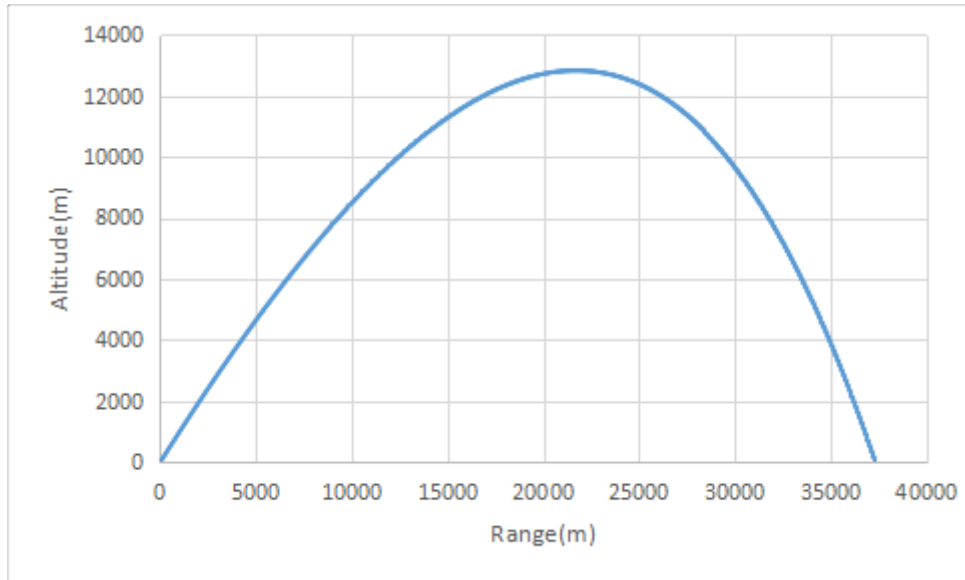


Figure 6.8: Altitude (m) vs Range (m)

From Figure 6.8, it's observed that the firing range of the projectile is 37800 m. The maximum height traveled by the projectile is 13000 m. The real time range of the gun is 38000 m. Therefore the error in the range is about 0.5%.

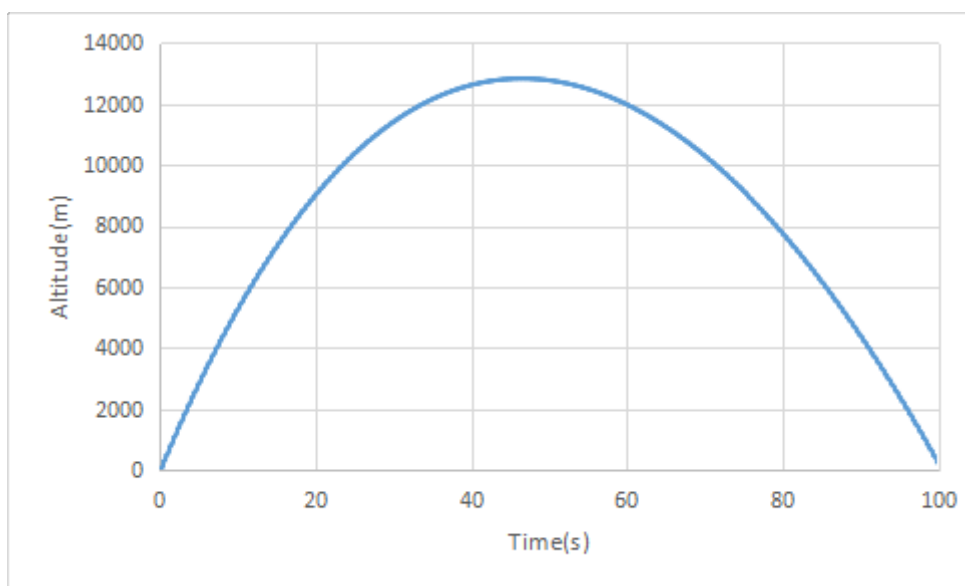


Figure 6.9: Altitude (m) vs Time (s)

From Figure 6.9, it is observed that the shell reaches a maximum height of 13000 m in 45 sec and after that the shell loses its momentum about y axis and falls down because of gravity.

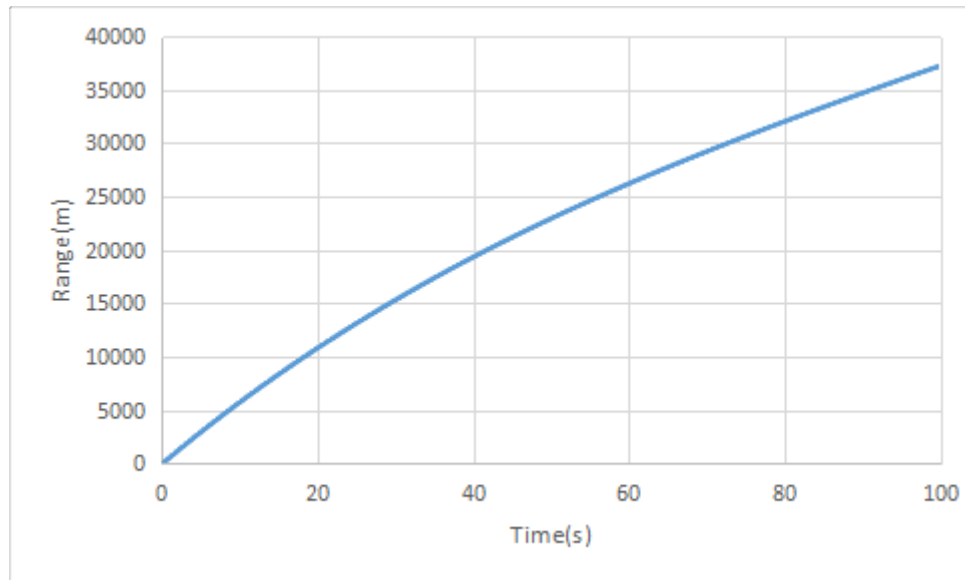


Figure 6.10: Range (m) vs Time (s)

From Figure 6.10, it is observed that the range of the projectile increases in a parabolic way. The reason behind this phenomenon is that the drag force acting on the projectile is a function of the square of the velocity at each component. The projectile travels up to a distance of 37800 m in 100 secs.

According to classical mechanics when an object is fired at an angle the velocity component of the projectile remains constant throughout the journey. Whereas if by observing the above figure the velocity of the projectile decreases as the time increases. The reason behind this phenomenon is because of the drag force acting against the motion of the projectile. When the shell hits the target the horizontal velocity component of the shell is around 260 m/s.

From Figure 6.12, it's clearly observed that as the projectile travels against gravity (the positive sign shows that the projectile is traveling in the upward direction) the vertical velocity keeps on decreasing and becomes zero at the peak at 45 secs. After the projectile loses its vertical momentum at the apogee it falls down due to the gravita-

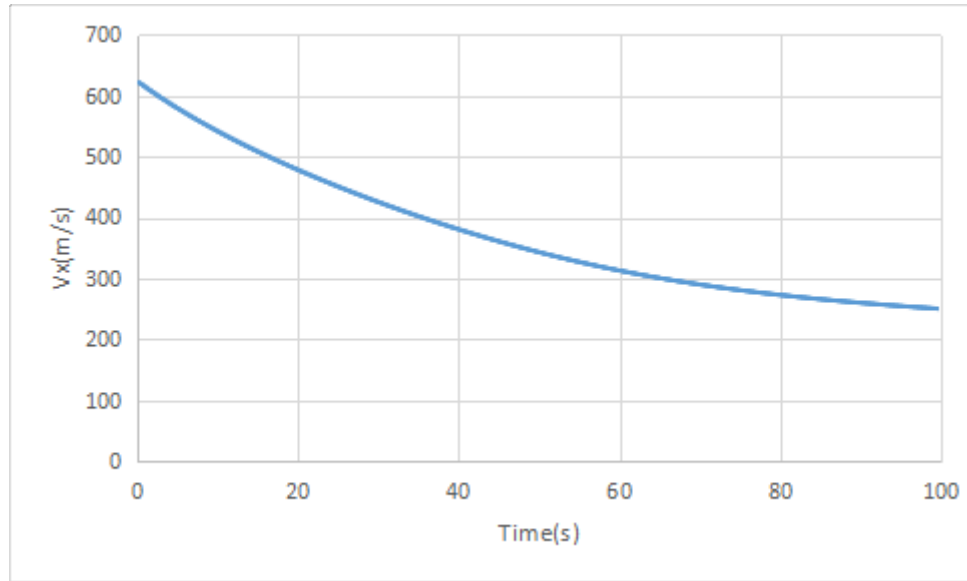


Figure 6.11: V_x (m/s) vs Time(s)

tional force (the negative sign shows that the projectile is travelling in the downward direction). As the projectile touches the ground the vertical velocity is around 450 m/s. The projectile is unable to attain the initial velocity at the firing site because of air resistance.

The drift force acting on the project is because of cross wind and the gyroscopic force which makes the projectile move away from the target. From the above graph it's observed that the lateral distance traveled by the shell increases because of the overturning moment. The maximum deflection of the shell 0.078 m with an error of 9.7%. From Figure 6.14, initially the yaw angle increases with respect to time because the torque acting on the shell is more than the overturning moment and further it falls down as the spin rate decreases and the overturning moment predominates.

From Figure 6.15, the angle of attack decreases till the point of apogee due to the decrease in velocity about the vertical axis. As the projectile reaches the apogee it becomes zero. When the projectile falls down due to gravity the angle of attack further increases due to increase in velocity about the vertical axis and finally hits the target around 50 degree and the nose points downward.

From Figure 6.16, it can be observed that the rate of spin decreases with time up to

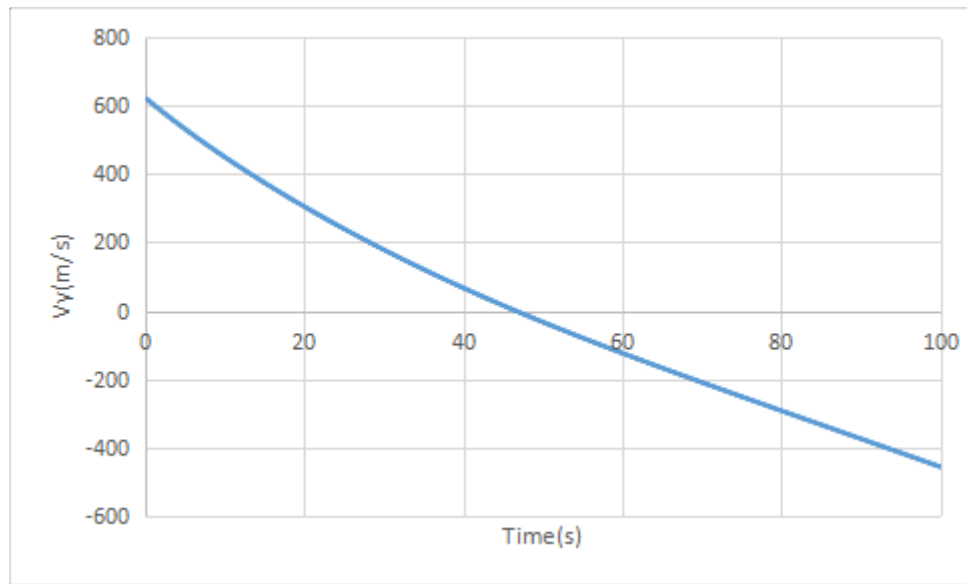


Figure 6.12: V_y (m/s) vs Time(s)

a certain time because spin damping. After 55sec the spin rate increase to 10000rad/s due to increase in the net velocity of the projectile.

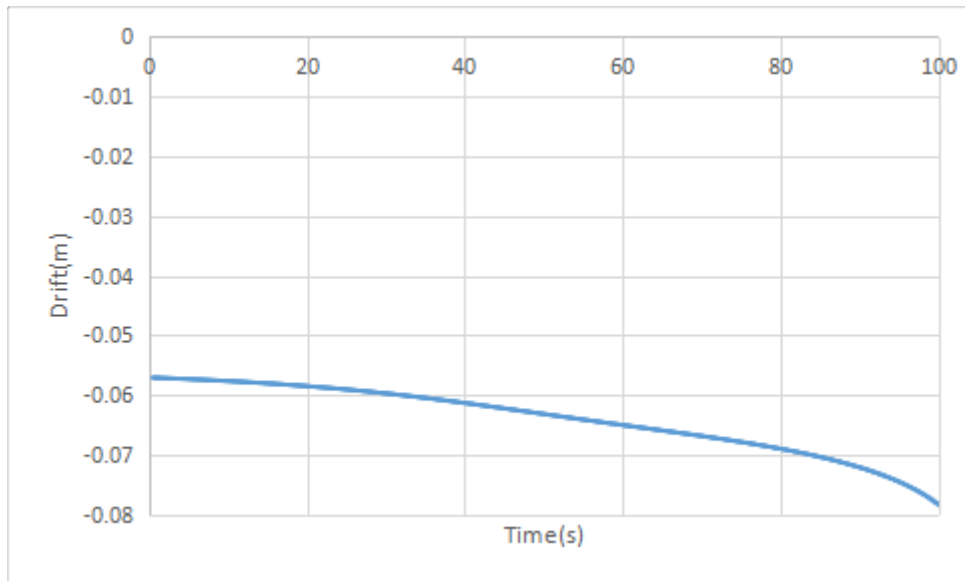


Figure 6.13: Lateral Deflection of the projectile (m) vs Time (s)

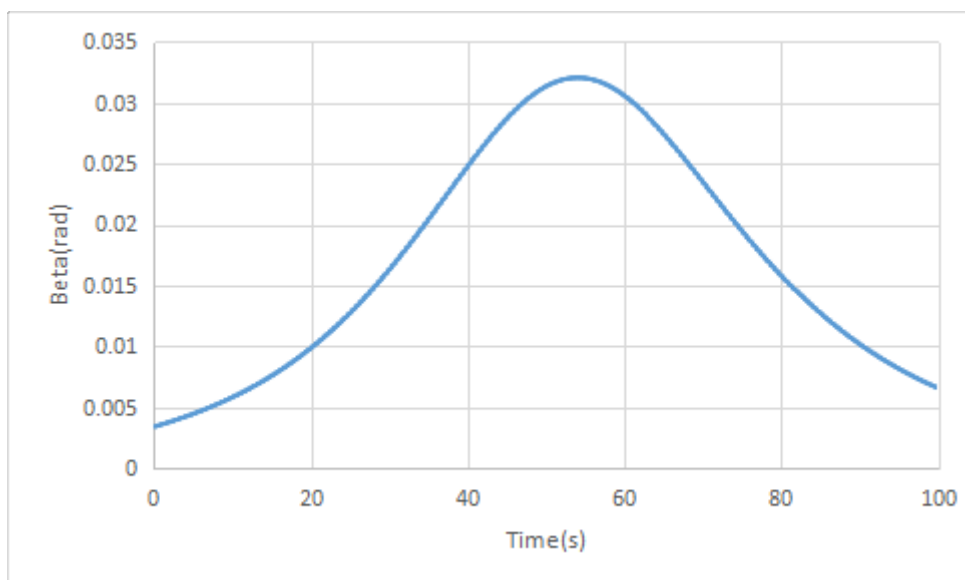


Figure 6.14: Yaw Repose (rad) vs Time (s)

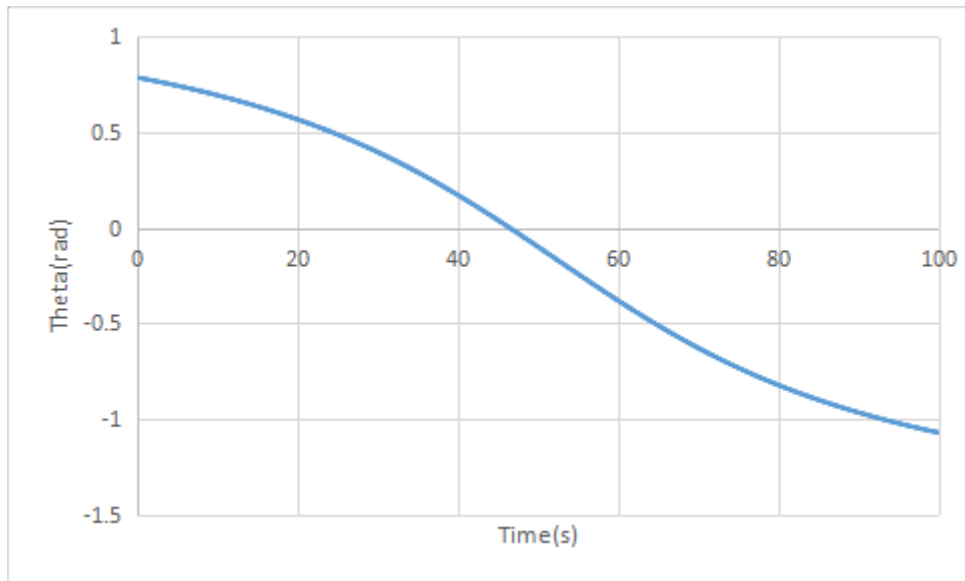


Figure 6.15: Angle of attack(rad) vs Time(s)

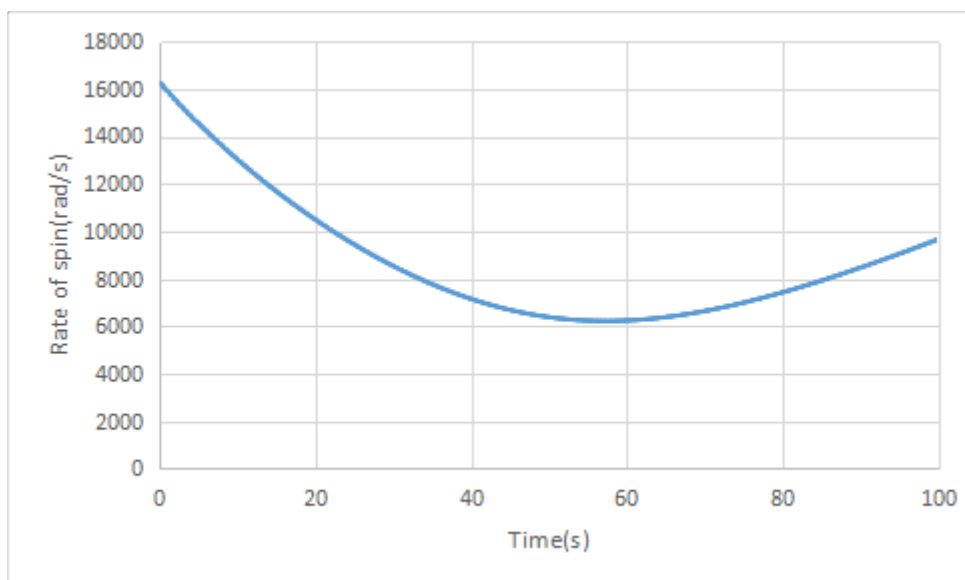


Figure 6.16: Rate of spin(rad/s) vs Time(s)

CHAPTER 7

CONCLUSION

The range of the artillery shell of 155 mm diameter is calculated and predicted using numerical methods. The equations governing the trajectory in 6 Degrees of Freedom have been discussed. The coefficient of drag of the artillery shell at different Mach Numbers and altitudes have been simulated and verified where there is change in density and pressure. Cubic curve fit is been used to compute the trajectory.

REFERENCES

1. Walter B. Sturek, CharlesJ. Nietubicz,t Jubaraj Sahu, and Paul Weinacht (1994), "Applications of Computational Fluid Dynamics to the Aerodynamics of Army Projectiles", *Journal of Spacecraft and Rockets*.
2. G. R. Cooper and Mark Costello (2011), "Trajectory Prediction of Spin-Stabilized Projectiles with a Liquid Payload", *Journal of Spacecraft and Rockets*, Vol. 48, No. 4.
3. A. Elsaadany, YI Wen, (2014), "Accurate Trajectory Prediction for Typical Artillery Projectile", *33rd Chinese Control Conference*.
4. Ryan F. Hooke, "The mathematical modelling of projectile trajectories under the influence of environmental effects", *University of New South Wales*. Canberra, Australian Defence Force Academy.
5. M.E. Wessam, "Z.H. Chen Firing Precision Evaluation For Unguided Artillery Projectile", *International Conference on Artificial Intelligence and Industrial Engineering*.
6. M. Khalil, H. Abdalla and O. Kamal (2009), "Trajectory Prediction for a Typical Fin Stabilized Artillery Rocket", *13th International Conference on Aerospace Science and Aviation Technology*.
7. K.K. Chand and H.S. Panda (2007), "Mathematical Model to Simulate the Trajectory Elements of an Artillery Projectile Proof Shot", *Defence Science Journal*, Vol. 57, No. 1.
8. Robert L. McCoy (1998), "Modern Exterior Ballistics", *4th edition*, Schiffir Publishing Ltd., 1998.
9. Bernard Etkin (1972), "Dynamics of Atmospheric Flight", *John Wiley & Sons*.